

MDPI

Article

Analysis of the Influence of Different Reference Models on Recovering Gravity Anomalies from Satellite Altimetry

Yu Han ¹, Fangjun Qin ¹, Hongwei Wei ^{1,*}, Fengshun Zhu ^{2,3} and Leiyuan Qian ¹

- College of Electrical Engineering, Naval University of Engineering, Wuhan 430033, China; d23381103@nue.edu.cn (Y.H.); haig2022@126.com (F.Q.); qian_leiyuan@163.com (L.Q.)
- State Key Laboratory of Geodesy and Earth's Dynamics, Innovation Academy for Precision Measurement Science and Technology, Chinese Academy of Sciences, Wuhan 430071, China; zhufengshun23@mails.ucas.ac.cn
- College of Earth and Planetary Sciences, University of Chinese Academy of Sciences, Beijing 100049, China
- * Correspondence: weihongweier@nudt.edu.cn

Abstract: A satellite altimetry mission can measure high-precision sea surface height (SSH) to recover a marine gravity field. The reference gravity field model plays an important role in this recovery. In this paper, reference gravity field models with different degrees are used to analyze their effects on the accuracy of recovering gravity anomalies using the inverse Vening Meinesz (IVM) method. We evaluate the specific performance of different reference gravity field models using CryoSat-2 and HY-2A under different marine bathymetry conditions. For the assessments using 1-mGal-accuracy shipborne gravity anomalies and the DTU17 model based on the inverse Stokes principle, the results show that CryoSat-2 and HY-2A using XGM2019e_2159 obtains the highest inversion accuracy when marine bathymetry is less than 2000 m. Compared with the EGM2008 model, the accuracy of CryoSat-2 and HY-2A is improved by 0.6747 mGal and 0.6165 mGal, respectively. A weighted fusion method that incorporates multiple reference models is proposed to improve the accuracy of recovering gravity anomalies using altimetry satellites in shallow water. The experiments show that the weighted fusion method using different reference models can improve the accuracy of recovering gravity anomalies in shallow water.

Keywords: gravity anomaly; satellite altimetry; reference gravity fields; marine bathymetry; accuracy evaluation



Citation: Han, Y.; Qin, F.; Wei, H.; Zhu, F.; Qian, L. Analysis of the Influence of Different Reference Models on Recovering Gravity Anomalies from Satellite Altimetry. *Remote Sens.* 2024, 16, 3758. https://doi.org/10.3390/rs16203758

Academic Editor: Chung-Ru Ho

Received: 19 August 2024 Revised: 5 October 2024 Accepted: 7 October 2024 Published: 10 October 2024



Copyright: © 2024 by the authors. Licensee MDPI, Basel, Switzerland. This article is an open access article distributed under the terms and conditions of the Creative Commons Attribution (CC BY) license (https://creativecommons.org/licenses/by/4.0/).

1. Introduction

The Earth's gravity field is one of the inherent characteristics of the geophysical environment. Its complexity and dynamics profoundly affect many physical processes of the Earth and its adjacent space [1]. The marine gravity field is an important part of the Earth's gravity field. Accurate marine gravity field information has a significant impact on the theoretical research of geoid refinement, internal mass distribution of the Earth, geodynamics, and seismology. In addition, the marine gravity field is also crucial for engineering applications, such as marine mineral resource development, satellite orbit determination, inertial navigation technology, and gravity matching navigation [2–6].

The acquisition methods of the marine gravity field mainly include satellite gravity measurement, altimetry, airborne gravity, and shipborne gravity measurement. Satellite gravity measurement is good at capturing long-wave information, while satellite altimetry contains medium- and short-wave information of the marine gravity field. Airborne gravity measurements efficiently gather high-precision, medium- to short-wave information but are costly and limited in large-scale coverage [7]. Shipborne methods, offering high spatial resolution and accuracy, record all bands of information and have improved with advancements in atomic ocean gravimeters, now reaching sub-mGal accuracy (1 mGal = 1×10^{-5} m/s²) [8–12]. Although the shipborne gravity measurement method

has been applied for nearly a hundred years, there are still large areas that have not been surveyed using shipborne gravity measurement methods. However, altimetry satellites developed in recent decades have brought the spatial resolution and accuracy of marine gravity data close to those of shipborne gravity measurements in some regions of the global oceans [13–16]. Most of the current large-scale marine gravity field models primarily rely on satellite altimetry. Satellite altimetry technology provides more than 60% of the global sea surface height data, effectively addressing issues such as significant human and financial costs, sparse data acquisition, poor repetition periodicity, and the inaccessibility of remote marine areas [17,18].

Using altimeter data to obtain the marine gravity field involves inverting the geoid fluctuations from satellite height data and then applying the corresponding inversion algorithm to derive the marine gravity field [18-21]. Many scholars have harnessed altimeter data to develop high-precision gravity field models, benchmarking their accuracy against shipborne gravity measurements. Zaki [22] conducted a comparative analysis of the DTU13 and SS V23.1 altimeter-derived gravity models in the Red Sea, utilizing shipborne gravity data as a reference. The findings indicated that while both models demonstrated comparable accuracy, DTU13 exhibited a marginally superior performance with a mean deviation of -2.40 mGal and a standard deviation of 8.71 mGal. Bao Lifeng [23] assessed the efficacy of altimeter-derived gravity field models in the offshore and coastal marine regions of China. The analysis revealed that the root mean square (RMS) deviations exceeded 7 mGal in offshore areas and ranged from 9.5 to 10.2 mGal along the coastlines. Wang Bo [24] conducted a comprehensive multi-attribute analysis in the South China Sea, evaluating the accuracy and spatial resolution of three different marine gravity field models (DTU17, SS V32.1, and SDUST) against two sets of shipborne gravity data. The study found that the RMS between these models and shipborne measurements varied, with ranges of 3.48 to 7.01 mGal, 3.38 to 6.80 mGal, and 2.64 to 6.83 mGal, respectively. Annan and Wan [25] developed products that deflect vertical and gravity anomalies for the Gulf of Guinea region, leveraging the data from five altimetry missions, including HY-2A. Their gravity anomaly product was found to exhibit comparable accuracy to DTU13, SS V28.1, and EGM2008. Notably, a comparison with shipborne gravity anomaly data that has undergone quadratic polynomial fitting correction indicates that the gravity anomaly product exhibits better accuracy at marine depths below 2000 m.

The key factors influencing the recovery of marine gravity fields from satellite altimetry encompass inversion theories and data characteristics [26]. At present, there are methods based on the Laplace equation [13], the inverse Vening Meinesz method [27,28], the inverse Stokes formula [29], and the least squares method [30]. Different methods have different accuracies of their inversion results. The diversity of the over 20 altimetry satellites globally, each with unique orbits and frequency bands, further contributes to these differing gravity inversions. Data retracking techniques involve empirical and function-based waveform resetting [31]. Additionally, the choice of reference gravity model, sea surface topography, and tidal model impacts the results. While extensive research exists on inversion theories, precise orbit determination, and multi-source data processing, the impact of remove–restore methods in gravity anomaly inversions remains understudied [1,32]. This paper focuses on analyzing the effect of different gravity field reference models on gravity anomaly inversions, employing the inverse Vening Meinesz method. We selected different gravity field reference models to analyze their effectiveness in recovering gravity fields from altimeter data and conducted a comparative analysis with the marine gravity model released by the Technical University of Denmark, as well as shipborne gravity measurement data.

2. Research Area and Data

2.1. Research Area

The study area is located between 140° E $\sim 150^{\circ}$ E and 20° N $\sim 30^{\circ}$ N, including part of the Mariana Trench, which is the deepest part of the ocean in the world. Because its

Remote Sens. 2024, 16, 3758 3 of 16

seabed topography is closely related to its gravity anomalies, the significant seabed terrain drop inevitably affects the accuracy of the altimeter-derived gravity anomalies. At the same time, this region contains more shipborne gravity data, so the region was selected for an evaluation of the influence of different reference models on altimeter-derived marine gravity anomalies. The seabed topography and ship survey trajectories within the study area are shown in Figure 1.

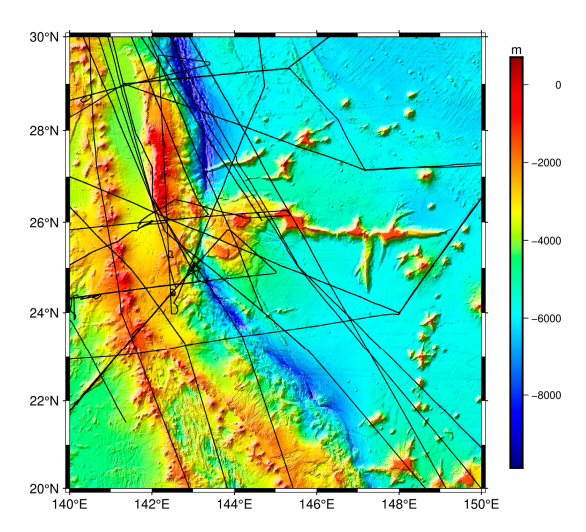


Figure 1. The seabed topography of the study area and shipborne gravity tracks (the black line is the shipborne tracks).

2.2. Data Description and Models

2.2.1. Satellite Altimetry Data

AVISO (Archiving, Validation and Interpretation of Satellite Oceanographic data, https://www.aviso.altimetry.fr, accessed on 1 July 2024) has released the along-track nontime-critical Level-2+ (L2P) products of version 4.0 [33], from which the sea surface height (SSH) data can be obtained. Detailed information on the altimeter data is shown in Table 1. HY-2A was launched in 2011 and is equipped with a dual-frequency altimeter (Ku-band and C-band) with an accuracy of 4 cm. The orbital inclination of HY-2A is 99.34°, and the orbital height is 971 km. The period was 14 days in the early stages, but it was adjusted to 168 days after the orbit change in 2016. The satellite remained in this geodetic mission (GM) orbit until 2020, accumulating data for over four years. CryoSat-2 was launched in 2010, and it is the first altimetry satellite equipped with a new Synthetic Aperture Interferometric Radar Altimeter (SARAL). The satellite can perform delayed Doppler observations in one direction during flight, which means that the resolution is several times higher than that of traditional altimetry, reaching about 300 m. The ground tracks of the satellite in the study area are shown in Figure 2. The ground tracks of CryoSat-2 are denser than those of HY-2A/GM because the period of CryoSat-2 is 369 days, which is more than twice the period of HY-2A/GM. In the process of computing the SSH from the altimeter data, adjustments were needed for dry and wet tropospheric effects, ionospheric variations, oceanic and polar tides, Earth solid tides, dynamic atmospheric factors, and sea state biases, ensuring accuracy and reliability of the final result.

Table 1. Information on the altimeter data.

Satellite	CryoSat-2	HY-2A/GM
Product	L2P	L2P
Inclination (°)	92	99.34
Cycle Duration (days)	369	168
Time Period	cycle 007-cycle 130	cycle 067–cycle 288

Remote Sens. 2024, 16, 3758 4 of 16

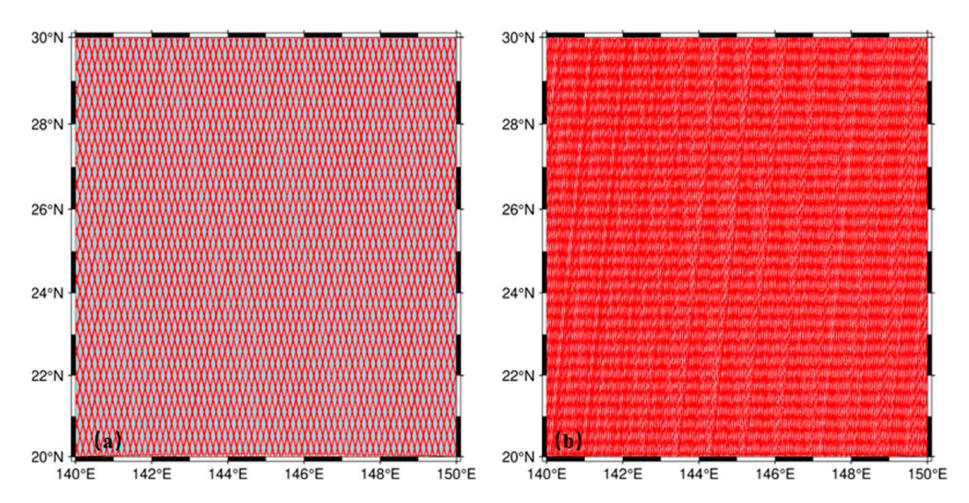


Figure 2. Ground track density of the altimeter data. (a) HY-2A. (b) CryoSat-2.

2.2.2. Shipborne Gravity Data

Shipborne data were provided by the Japan Agency for Marine-Earth Science and Technology (JAMSTEC, https://www.godac.jamstec.go.jp, accessed on 1 July 2024). These data include quality-controlled absolute gravity measurements and free-air gravity anomalies. The absolute gravity data are a combination of relative gravity data measured by a shipboard gravity meter and absolute gravity data from the ports during departure and arrival. Drift corrections and the Eotvos corrections were performed before converting the data into absolute gravity data. As part of quality control, data with low reliability were removed. As shown in Figure 1, this paper selected 12 cruises in the study area, a total of 253,911 gravity points. These data were collected between 2005 and 2008, and specific information about the survey lines are shown in Table 2.

Cruise	Period (UTC)	Max	Min	Number	Gravimeter	Accuracy
KR05-01	05/01/2005~24/01/2005	126.9	-264.9	4511		
KR05-14	05/10/2005~18/10/2005	115.8	-249.7	5389		
KR05-16	11/11/2005~04/12/2005	134.6	-209.3	10,612		
KR05-17	10/12/2005~25/12/2005	151.6	-224.6	4750	01 1 1	
KR06-01	05/01/2006~26/01/2006	129.9	-99.0	9488	Shipboard gravimeter:	
KR06-07	05/07/2006~26/07/2006	371.8	-263.5	69,821		1.0
KR06-12	13/09/2006~22/09/2006	111.6	-166.9	10,926	KSS 31Portable	1.0
KR06-14	29/10/2006~19/11/2006	193.6	-249.0	37,468	gravimeter: CG-3M	
KR06-15 Leg1	24/11/2006~26/11/2006	124.8	-236.2	7791		
KR06-16	15/12/2006~27/12/2006	133.6	-14.4	4738		
KR07-03	03/03/2007~29/03/2007	212.5	-214.3	81,603		
KR07-16	26/11/2007~01/12/2007	215.7	-116.3	6814		

Table 2. Statistics of the shipborne gravity data in the study area (unit: mGal).

2.2.3. Marine Gravity Anomaly Model

The marine gravity field model published by the Technical University of Denmark is one of the high-precision models available. The latest version of the models is DTU17, which incorporates data from the CryoSat-2, Jason-2, and SARAL/AltiKa satellites. The notable enhancement in the wavelength signals within the 10 to 15 km range in the new version uncovers novel gravity field structures and bathymetric features. Figure 3 illustrates the gravity anomalies of DTU17 in the study area.

Remote Sens. 2024, 16, 3758 5 of 16

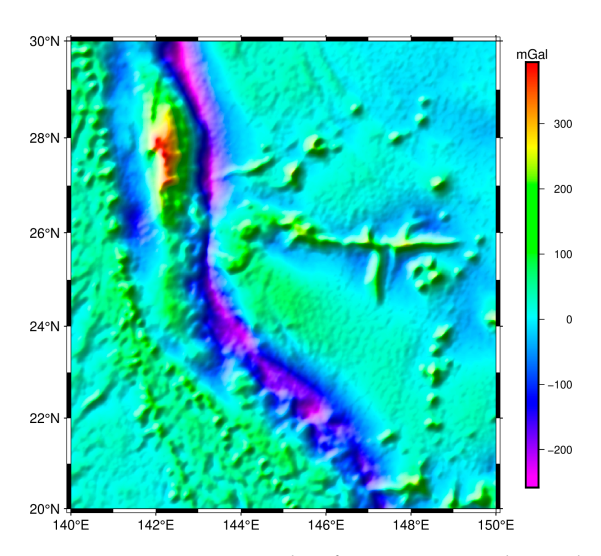


Figure 3. Gravity anomalies from DTU17 in the study area.

2.2.4. Reference Gravity Field Model

Earth's reference gravity field models are utilized in the remove–restore method. This paper selects six reference gravity field models: HUST-Grace2016s, WHU-SWPU-GOGR2022S, EGM2008, XGM2019e_2159, EIGEN-6C4, and SGG-UGM-2. The spherical harmonic coefficients for these models can be downloaded from the International Centre for Global Earth Models (ICGEM, https://icgem.gfz-potsdam.de/tom_longtime, accessed on 1 July 2024). Information regarding the reference gravity field models is presented in Table 3.

Model	Year	Degree	Data	Institution
HUST-Grace2016s	2016	160	Grace	HUST
WHU-SWPU- GOGR2022S	2023	300	Goce, Grace	WHU/SWPU
SGG-UGM-2	2020	2190	Altimetry, EGM2008, Goce, Grace	WHU
EGM2008	2008	2190	Altimetry, Ground data, Grace	NGS/NASA
EIGEN-6C4	2014	2190	Altimetry, Ground data, Goce, Grace, Lageos	GFZ/GRGS
XGM2019e_2159	2019	2190	Altimetry, GOCO06s, Ground data, topography	GFZ

Table 3. Information on the different reference gravity field models.

3. Method

3.1. Shipborne Gravity Preprocessing Method

The shipborne gravity data provided by JAMSTEC included absolute gravity data and free-air anomalies. We only use the free-air anomalies here. The original absolute gravity data has been corrected by drift correction and the Eotvos effect, and some outliers have been deleted. However, there are still some long-wave errors in the data, so it is necessary to pre-process the data to facilitate the verification of the gravity field derived from the altimeter. We determined the mean value and standard deviation of the free-air anomalies of each cruise and removed any gross differences contained in the data according to the principle of triple sigma. The number of points was reduced from 253,911 gravity points to 250,491, and 3420 points were eliminated, accounting for 1.34%. In addition, with reference to [34], we calculated the average difference between the reference gravity field and the shipborne gravity data after removing the gross difference in the data and added the average difference to the shipborne data after removing any other differences to obtain the adjusted shipborne data.

Remote Sens. 2024, 16, 3758 6 of 16

3.2. Processing Method of the Altimeter Data

We chose to invert the deflection of vertical (DOV) using the altimeter data and further use the DOV to invert the gravity anomalies in the study area. This method reduces long-wave errors including atmospheric propagation errors, ocean circulation errors, tidal errors, and so on. In addition, the geoid gradient encompasses abundant high-frequency information, which is conducive to high-resolution inversion of the marine gravity field. Therefore, many scholars have used this method for gravity field inversion [28,34,35]. Hwang derived the inverse Vening Meinesz formula, which converts DOV into gravity anomalies by utilizing the gradient of the H function, based on the spherical harmonic representations of the Earth's disturbing potential and its associated functions. Additionally, the distinction in the application of one-dimensional Fast Fourier Transform (1D FFT) for calculating spherical latitude was taken into account, which led to a more rigorous theoretical foundation [28]. We have also adopted this method, with the specific process illustrated in Figure 4. Subsequently, we will provide a concise introduction to the underlying principles of this section.

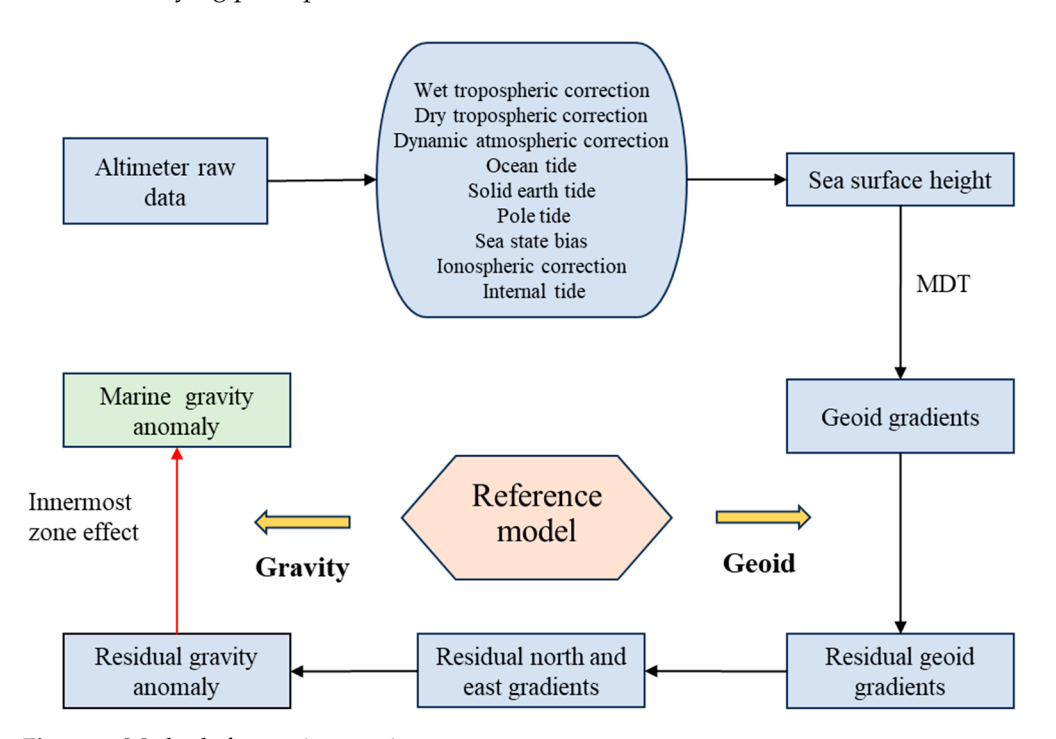


Figure 4. Methods for marine gravity recovery.

We performed atmospheric corrections and a series of geophysical corrections on the original altimeter data to calculate the *SSH*. The mean dynamic topography (*MDT*) was deducted from the *SSH* to obtain the geoid height. The along-track geoid slope can be calculated by using the adjacent geoid height along the satellite track,

$$\partial h = -\frac{N_j - N_i}{d},\tag{1}$$

where $N_i = SSH_i - MDT_i$ is the spherical distance between substellar points i and points j. The azimuth angle α_{ij} between points i and j can be calculated by

$$\tan \alpha_{ij} = \frac{\cos \varphi_j \sin(\lambda_j - \lambda_i)}{\cos \varphi_i \sin \varphi_j - \sin \varphi_i \cos \varphi_j (\lambda_j - \lambda_i)}$$
(2)

The residual along-track geoid slope can be obtained by subtracting the geoid slope from the reference gravity model from the along-track geoid slope. In order to facilitate subsequent use of one-dimensional Fast Fourier Transform (1D FFT), it is necessary to

Remote Sens. 2024, 16, 3758 7 of 16

calculate the DOV after gridding. Using the Least Squares Collocation (LSC) method, the residual north and east components of the DOV are calculated using the residual along-track geoid slope and the covariance matrix. In this paper, a detailed derivation of the formula is not performed; the interested reader is referred to [20,36,37].

On a sphere with a specific radius, the gravity anomaly can be expressed as follows:

$$\Delta g(\phi, \lambda) = \left(-\frac{\partial T}{\partial r} - \frac{2}{r}T\right)|_{r=R} = \gamma_0 \sum_{n=2}^{\infty} (n-1) \times \sum_{m=0}^{n} \sum_{\alpha=0}^{1} C_{nm}^{\alpha} Y_{nm}^{\alpha}(\phi, \lambda)$$
(3)

where r, ϕ and λ are spherical coordinates, and C_{nm}^{α} is the potential coefficient. Y_{nm}^{α} is a completely regularized spherical harmonic function. γ_0 is the average gravity. T is the disturbing potential.

By introducing a spherical harmonic function, the Green formula, and a kernel function and using the relationship between spherical triangles, Professor Hwang finally deduced the following form of gravity anomaly [27]:

$$\Delta g(p) = \frac{\gamma_0}{4\pi} \iint_{\sigma} H' \cdot \left(\xi_q \cos \alpha_{qp} + \eta_q \sin \alpha_{qp} \right) d\sigma_q \tag{4}$$

where p and q are two points on the sphere. ξ_q and η_q are the north and east components of the DOV. The kernel function H' can be expressed as follows:

$$H' = \frac{dH}{d\psi_{pq}} = -\frac{\cos\frac{\psi_{pq}}{2}}{2\sin^2\frac{\psi_{pq}}{2}} + \frac{\cos\frac{\psi_{pq}}{2}\left(3 + 2\sin\frac{\psi_{pq}}{2}\right)}{2\sin\frac{\psi_{pq}}{2}\left(1 + \sin\frac{\psi_{pq}}{2}\right)}$$
(5)

When the distance between p and q becomes 0, the kernel function will be singular. At this time, we need to further consider the innermost zone effect. The specific formula is as follows:

$$\Delta g(\text{inner}) = \frac{1}{2} s_0 \cdot \gamma_0 \cdot (\xi_x + \eta_y) \tag{6}$$

where s_0 is the size of the innermost zone, ξ_x is the north derivative of ξ , and η_y is the east derivative of η .

4. Results and Discussion

4.1. Different-Degree Reference Gravity Models

Different reference gravity models have different effects on the remove–restore method. In this section, HUST-Grace2016s, WHU-SWPU-GOGR2022S, and EGM2008 are used as reference gravity models to analyze the accuracy of the gravity anomalies derived from the altimeter by IVM. Based on the above three different reference gravity models in the study area, the gravity anomalies inverted from HY-2A and CryoSat-2 are illustrated in Figures 5 and 6, respectively. Specifically, (a), (b), and (c) represent the gravity anomalies inverted using the aforementioned three different reference gravity models, while (d), (e), and (f) show the differences between the altimeter-derived gravity anomalies and those of DTU17. The altimeter-derived gravity anomalies are validated using DTU17, and the error results are shown in Table 4.

Remote Sens. 2024, 16, 3758 8 of 16

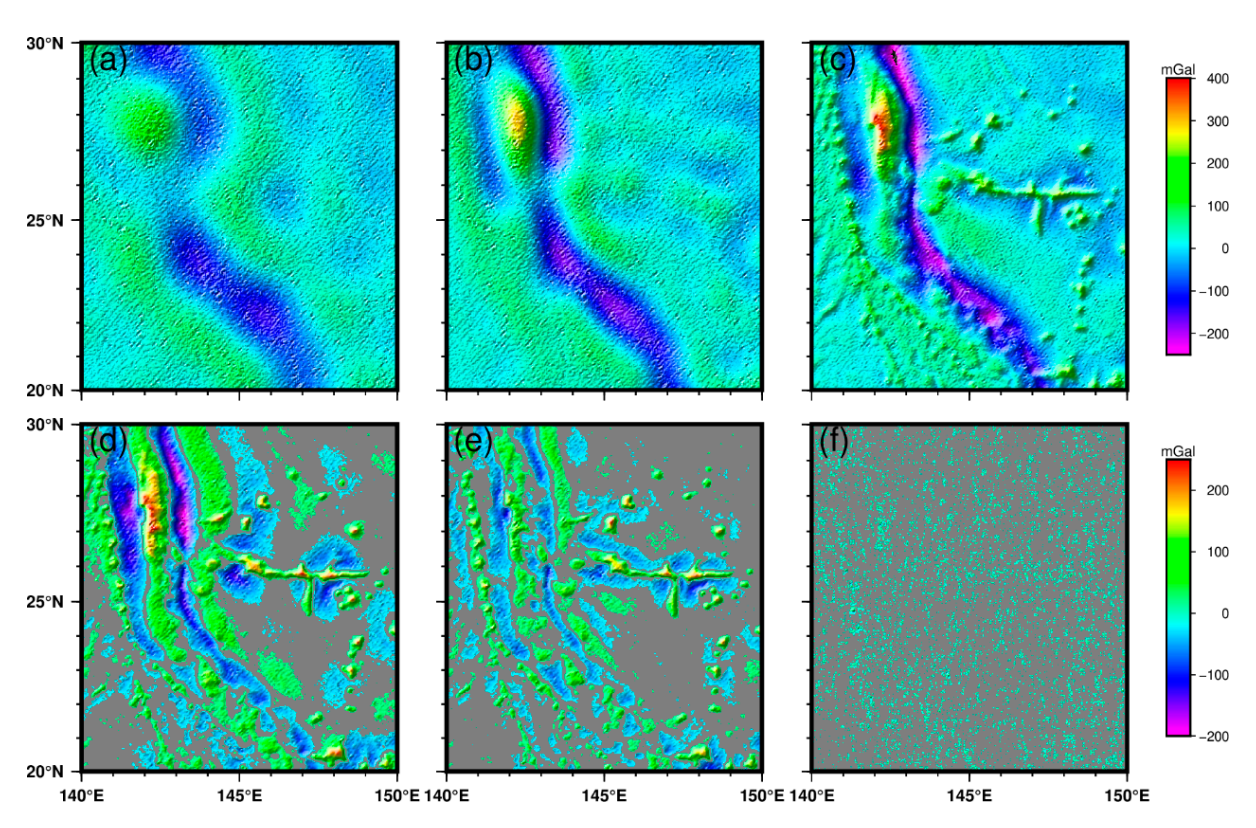


Figure 5. Gravity anomalies and error distribution from HY-2A. (**a–c**) Gravity anomalies derived from HUST-Grace2016s, WHU-SWPU-GOGR2022S, and EGM2008, respectively; (**d–f**) error between altimeter-derived gravity anomalies and DTU17, respectively.

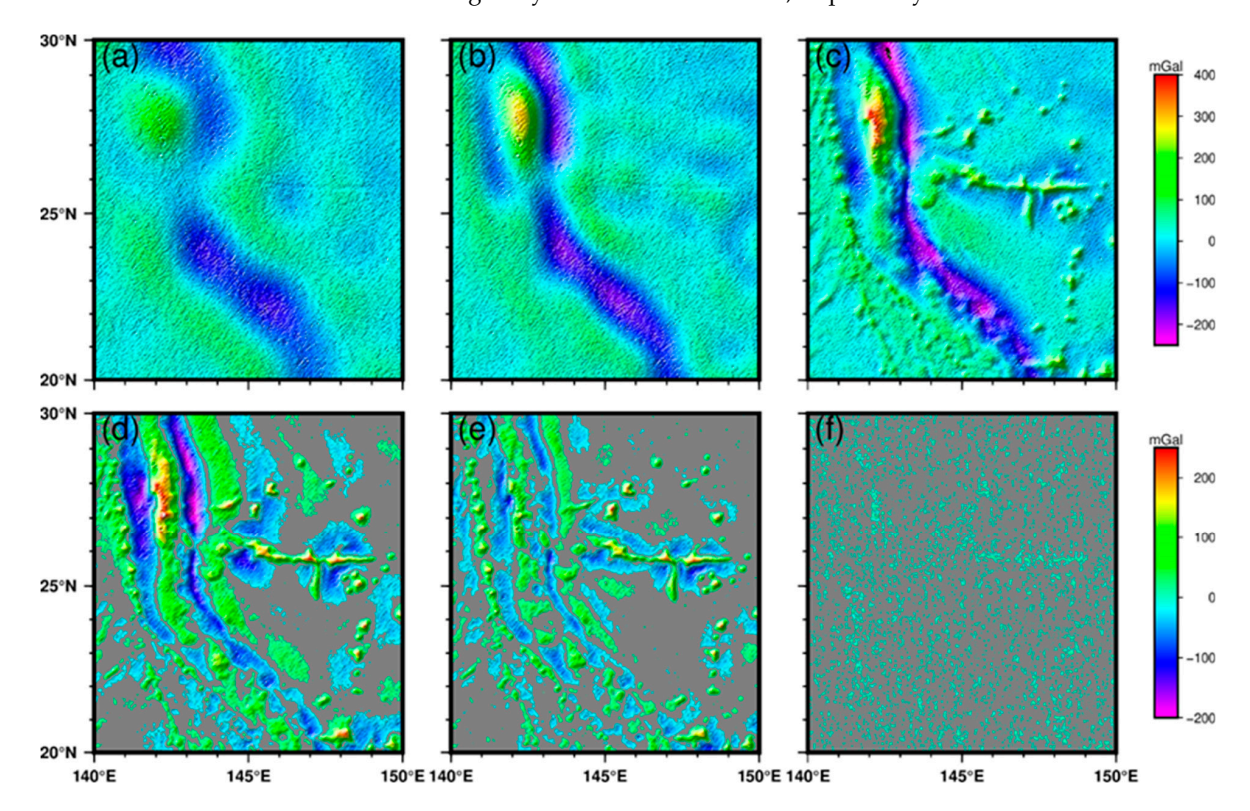


Figure 6. Gravity anomalies and error distribution from CryoSat-2. (a-c) Gravity anomalies derived from HUST-Grace2016s, WHU-SWPU-GOGR2022S, and EGM2008, respectively; (d-f) error between altimeter-derived gravity anomalies and DTU17, respectively.

Remote Sens. 2024, 16, 3758 9 of 16

Table 4. Statisti	cal information a	about differences	between DTU1	7 and	l altimeter-c	lerived	gravity
anomalies (unit:	mGal).						

Satellite	Reference Model	Min	Max	Mean	Std
	HUST-Grace2016s	-200.7411	280.2770	0.2918	49.2385
CryoSat-2	WHU-SWPU-GOGR2022S	-111.9221	236.5845	-0.0351	31.5660
	EGM2008	-49.5802	62.6038	0.0284	3.6133
	HUST-Grace2016s	-203.4208	255.7436	0.2904	49.2219
HY-2A	WHU-SWPU-GOGR2022S	-112.6769	232.8994	-0.0378	31.2331
	EGM2008	-52.9798	62.7806	0.0249	3.8634

From the diagram and Table 4, we can find that the low-degree reference gravity models have a great influence on the gravity anomalies derived from altimeter data. When using the HUST-Grace2016s (160-degree), the standard deviation (STD) of the gravity anomalies for both satellite types exceed 49 mGal. With the WHU-SWPU-GOGR2022S (300-degree), the STD is reduced to about 31 mGal, marking a certain degree of accuracy improvement. It can be found from the diagram that the accuracy of most areas exceeds 20 mGal. The verification results using DTU17 indicate that the highest accuracy in gravity anomaly recovery is achieved when utilizing the EGM2008 (2190-degree) model. The STDs of HY-2A and CryoSat-2 reach 4.4266 mGal and 3.8634 mGal, respectively, and the statistical indicators are also optimal. Consequently, when leveraging altimeter data for marine gravity field recovery, a high-degree gravity field model should be prioritized as the reference gravity field.

4.2. The Influence of the High-Degree Reference Model and Its Relationship with Marine Bathymetry

In order to analyze the influence of different high-precision reference models of the same degree, four high-degree reference gravity models—EGM2008, EIGEN-6C4, SGG-UGM-2, and XGM2019e_2159—are selected for analysis. EGM2008 was compared with DTU17 in the previous section. This section primarily focuses on analyzing the influence of the remaining three reference gravity field models. Based on these three reference gravity models, the gravity anomalies inverted by HY-2A and CryoSat-2 in the study area, as well as their differences from the DTU17 model, are presented in Figures 7 and 8.

The DTU17 and shipborne gravity data in the study area were used to verify the gravity anomalies inverted by HY-2A and CryoSat-2, and the error results are summarized in Table 5. From the perspective of the average error, the average errors in the gravity anomalies calculated by the four high-degree reference models are negligible, approaching zero. Figures 7 and 8 reveal that the distribution of gravity anomaly errors based on four different high-degree reference models is similar. Additionally, Table 5 reveals that the STD based on XGM2019e_2159 as the reference model is the smallest among the four reference gravity models. Specifically, when comparing the gravity anomalies inverted using HY-2A to those from DTU17 and shipborne data, the STDs are 3.7725 mGal and 4.4088 mGal, respectively. Similarly, for CryoSat-2 satellite data, the STDs compared to DTU17 and shipborne data are 3.5706 mGal and 4.1903 mGal, respectively. At the same time, we can find that in the same reference gravity model, the STD of CryoSat-2 is smaller than that of HY-2A, which also proves that the data quality of CryoSat-2 is slightly higher than that of HY-2A. In Figure 9, the error statistics pertaining to the gravity anomalies derived from the two types of satellites, HY-2A and CryoSat-2, in comparison to DTU17 are presented. Notably, within the error range of less than 2 mGal, the reference gravity models XGM2019e 2159 and EGM2008 exhibit the highest proportions of accuracy, whereas SGG-UGM-2 demonstrates the poorest performance.

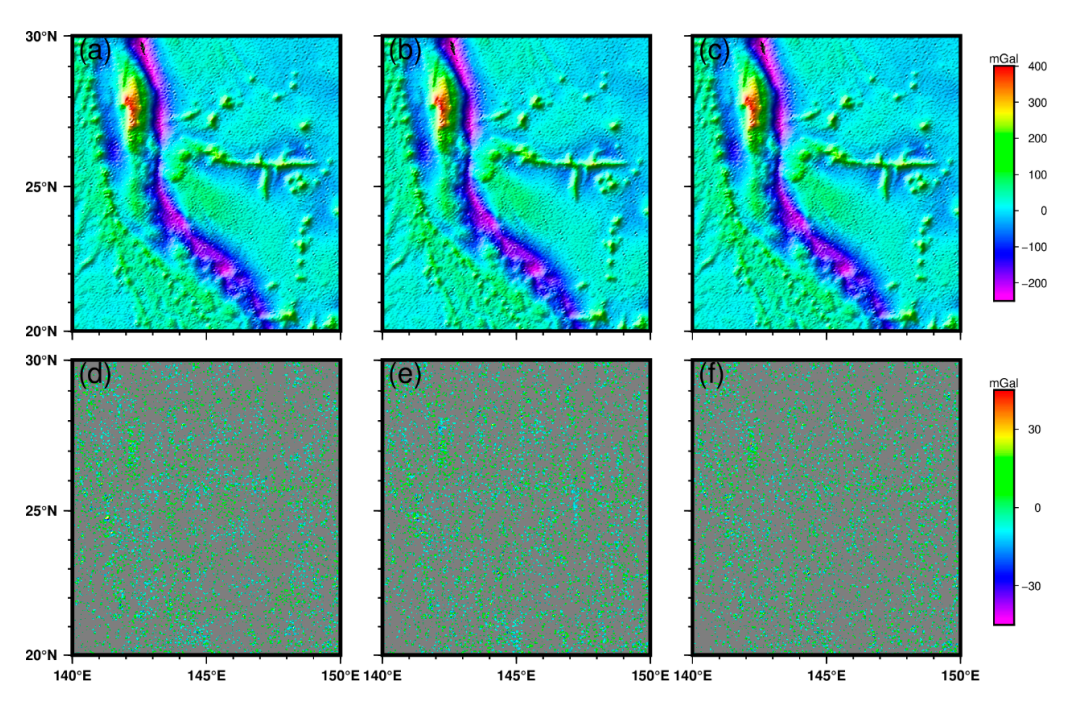


Figure 7. Gravity anomalies and error distribution from HY-2A. (a–c) Gravity anomalies derived from EIGEN-6C4, SGG-UGM-2, and XGM2019e_2159 respectively; (d–f) error between altimeter-derived gravity anomalies and DTU17, respectively.

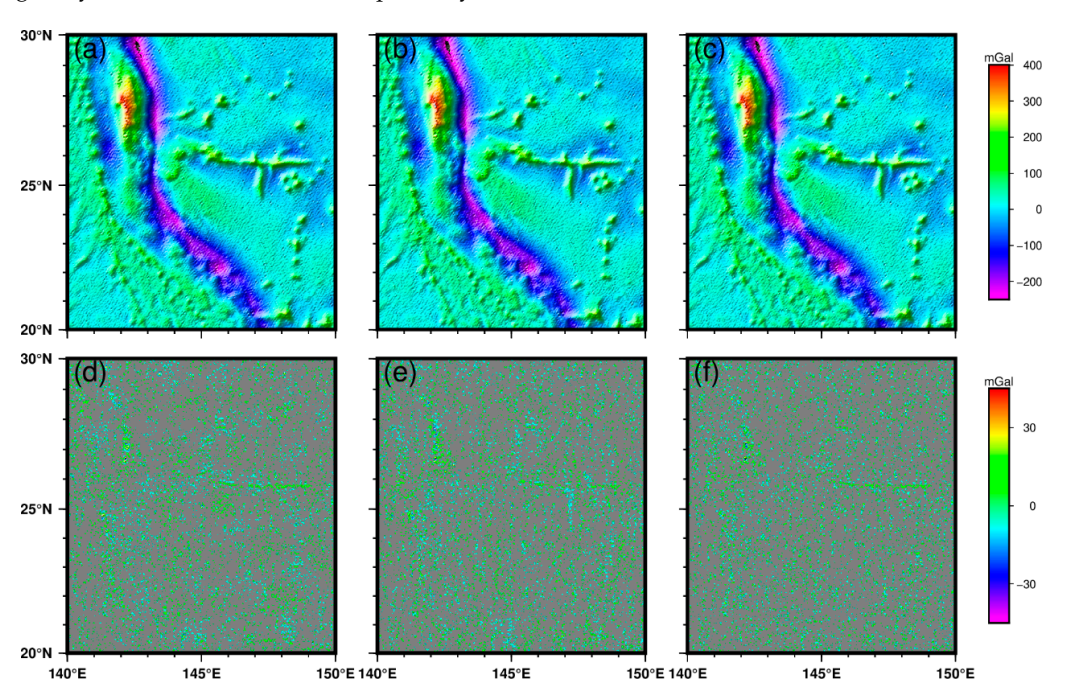


Figure 8. Gravity anomalies and error distribution from CryoSat-2. (**a–c**) Gravity anomalies derived from EIGEN-6C4, SGG-UGM-2, and XGM2019e_2159, respectively; (**d–f**) error between altimeter-derived gravity anomalies and DTU17, respectively.

Combined with the seabed topography, it can be found from Figures 7 and 8 that the distribution of altimeter-derived gravity anomaly errors is closely related to the marine bathymetry. We have calculated the relationship between the gravity anomaly error values, which were inverted using XGM2019e_2159, and the marine bathymetry in the study area, as shown in Figure 10. For marine depths greater than 6000 m, the STDs of the gravity anomalies inverted by HY-2A and CryoSat-2 are 3.4199 mGal and 3.3065 mGal, respectively. Conversely, when the marine depth is less than 6000 m, the STDs increase to

3.8357 mGal and 3.6184 mGal for HY-2A and CryoSat-2, showing an increase of 0.4158 mGal and 0.3119 mGal compared to the deeper waters. The results confirm a close relationship between inverted gravity anomalies and marine bathymetry. With the decrease in marine bathymetry, the accuracy of gravity anomalies also decreases. The accuracy of marine gravity anomalies is less reliable in shallower waters. The reduced accuracy in shallow waters is attributed to increased sea surface variations and altimeter tracking losses, which are caused by interference from onshore reflectors.

Table 5. Statistical information about the differences between the DTU17/shipborne data and gravity
anomalies derived from the altimeter (unit: mGal).

Satellite	Gravity Field	Reference Model	Min	Max	Mean	Std
		EGM2008	-52.9798	62.7806	0.0249	3.8634
	DTI 117	EIGEN-6C4	-49.8846	60.9428	0.0250	3.8290
	DTU17	SGG-UGM-2	-48.7438	56.7438	0.0183	3.9429
HY-2A		XGM2019e_2159	-45.5058	55.8648	0.0247	3.7725
111 2/1	Shipborne data	EGM2008	-23.4470	30.4806	0.1554	4.6973
		EIGEN-6C4	-23.7071	31.3502	0.3181	4.5655
		SGG-UGM-2	-24.6165	30.9431	0.2225	4.4339
		XGM2019e_2159	-24.3792	30.3459	0.1370	4.4088
		EGM2008	-49.5802	62.6038	0.0284	3.6133
	DELIAE	EIGEN-6C4	-45.0850	57.7311	0.0277	3.6382
	DTU17	SGG-UGM-2	-50.8154	41.2329	0.0212	3.7366
CryoSat-2		XGM2019e_2159	-59.4770	41.1555	0.0281	3.5706
		EGM2008	-27.5854	30.4129	-0.0026	4.3275
	Shipborne	EIGEN-6C4	-26.8541	31.8181	0.1434	4.2647
	data	SGG-UGM-2	-29.6454	30.5549	0.0531	4.1959
		XGM2019e_2159	-27.7187	28.9465	-0.0227	4.1903

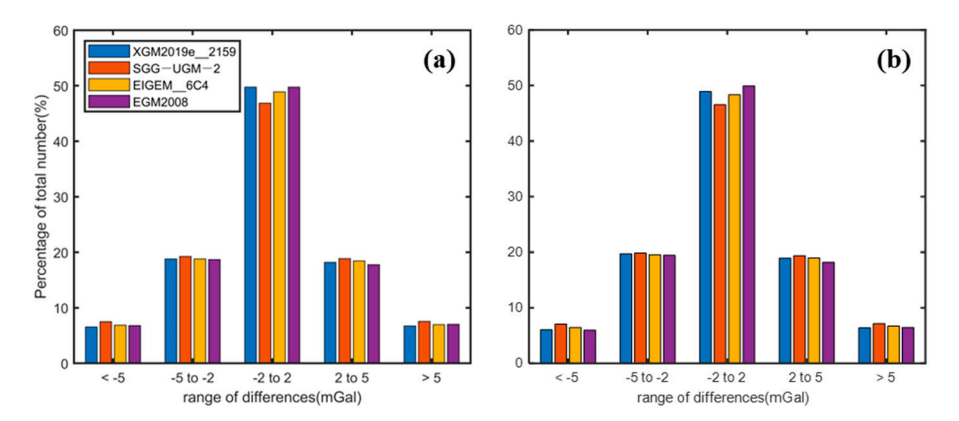


Figure 9. The error statistics between the gravity anomalies restored by different reference gravity models and DTU17. (a) HY-2A; (b) CryoSat-2.

Inspired by Figure 10 and reference [26], we further analyzed the influence of four different high-degree reference models on the recovery of marine gravity anomalies using altimeter data when the marine depth is greater than 6000 m and the marine depth is less than 2000 m. The specific results are shown in Tables 6 and 7, as well as Figure 11. Among the 57,381 points with a marine depth greater than 6000 m, we find that for both HY-2A and CryoSat-2, the STD of the gravity anomalies recovered by EGM2008 is the smallest compared with DTU17, at 3.3809 mGal and 3.2130 mGal, respectively. Compared with the EGM2008 model, the STD of gravity anomalies recovered by XGM2019e_2159 is about 0.1 mGal larger. Among the 20,186 points with a marine depth of less than 2000 m, we can find that the STD of gravity anomalies recovered using XGM2019e_2159 is the smallest;

HY-2A and CryoSat-2 are 4.6529 mGal and 5.0913 mGal, respectively. Compared with the EGM2008 model, the STD of the gravity anomalies recovered by the XGM2019e_2159 model is 0.6747 mGal and 0.6165 mGal smaller for HY-2A and CryoSat-2, respectively. Therefore, four high-degree reference models have a small effect on the recovery of gravity anomalies for satellites when the marine depth is more than 6000 m, while when the marine depth is less than 2000 m, the use of different reference gravity field models has a larger effect on gravity anomaly. The use of XGM2019e_2159 results in the highest accuracy of the gravity anomalies derived from altimeter data.

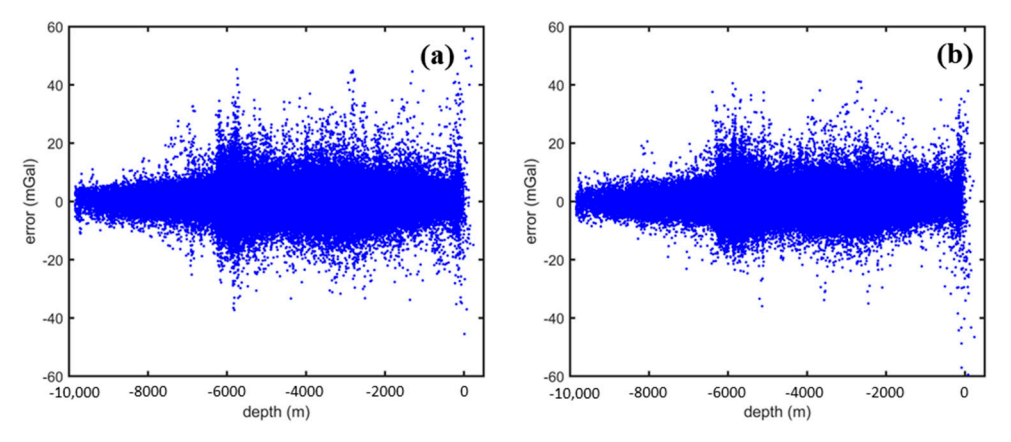


Figure 10. The relationship between gravity anomaly error and marine bathymetry. (a) The error between HY-2A and DTU17; (b) the error between CryoSat-2 and DTU17.

Table 6. Error statistics with DTU17 at marine bathymetry greater than 6000 m.

Satellite	Reference Model	<2 (%)	2~5 (%)	5~10 (%)	>10 (%)	STD (mGal)
	EGM2008	53.80	36.95	8.12	1.14	3.2130
C	EIGEN-6C4	51.79	38.10	9.03	1.08	3.2890
CryoSat-2	SGG-UGM-2	49.88	38.96	9.96	1.20	3.4065
	XGM2019e_2159	52.02	37.66	9.20	1.12	3.3065
	EGM2008	53.67	36.08	8.82	1.43	3.3809
HY-2A	EIGEN-6C4	52.30	37.17	9.18	1.35	3.3941
	SGG-UGM-2	49.92	38.14	10.48	1.46	3.5323
	XGM2019e_2159	52.26	37.07	9.29	1.38	3.4199

Table 7. Error statistics with DTU17 at marine bathymetry less than 2000 m.

Satellite	Reference Model	<2 (%)	2~5 (%)	5~10 (%)	>10 (%)	STD (mGal)
	EGM2008	36.83	36.32	20.74	6.11	5.3276
CryoSat-2	EIGEN-6C4	37.22	37.72	20.37	4.69	4.9708
Cryosat-2	SGG-UGM-2	36.45	38.44	20.43	4.68	5.0912
	XGM2019e_2159	40.04	39.08	17.28	3.61	4.6529
	EGM2008	36.43	36.16	20.54	6.87	5.7078
HY-2A	EIGEN-6C4	38.55	36.71	19.20	5.54	5.3721
	SGG-UGM-2	36.42	37.13	20.74	5.70	5.5554
	XGM2019e_2159	40.69	37.59	17.03	4.69	5.0913

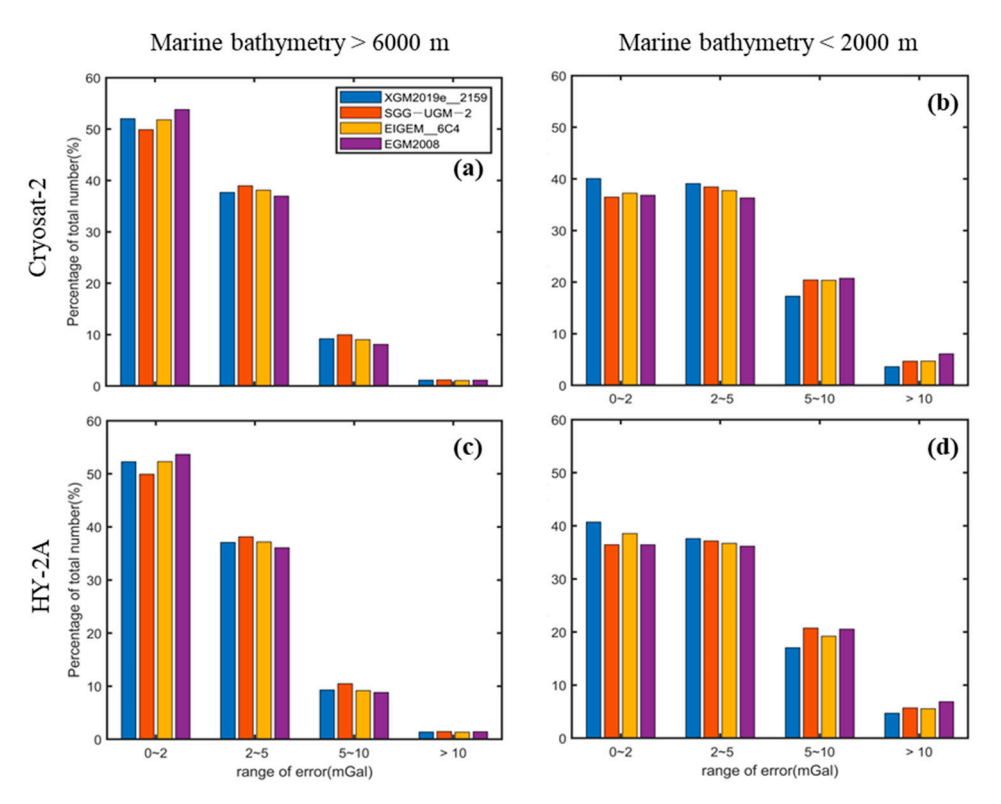


Figure 11. Statistics of errors between altimeter-derived gravity anomalies and DTU17 at different marine depths. (**a**,**b**) The errors in gravity anomaly inversion by CryoSat-2 for water depths exceeding 6000 m and those below 2000 m, respectively; (**c**,**d**) The errors in gravity anomaly inversion by HY-2A for water depths exceeding 6000 m and those below 2000 m, respectively.

4.3. Weighted Fusion of Different Reference Models

We analyzed the role of different reference models in the inversion of gravity anomalies using the IVM and found that these models have a certain impact on the resulting gravity anomalies, particularly in shallower waters. Consequently, we propose a weighted fusion method that incorporates multiple reference models to enhance the accuracy of recovering gravity anomalies in shallow waters. The weight assigned to each reference model is inversely proportional to the square of the STD of the error between that model and the DTU17:

$$P_i = \frac{1}{\delta_i^2} \tag{7}$$

Based on the STD between DTU17 and altimeter-derived gravity anomalies, we assigned weights to different reference models for marine areas with depths less than 2000 m. The results are presented in Table 8. Among them, XGM2019e_2159 had the highest weight proportion, accounting for 28.78% and 28.30% in CryoSat-2 and HY-2A, respectively, followed by EIGEM-6C4, and EGM2008 had the lowest proportion. The accuracy evaluation of the weighted fusion gravity anomalies is shown in Table 9. The STD for CryoSat-2 is reduced to 4.6214 mGal, and for HY-2A, it is reduced to 5.0686 mGal. The fusion result is better than that obtained using a single reference model, demonstrating a notable improvement in the accuracy of gravity anomalies recovered from altimeter data in shallow water areas.

Satellite	Component	Average STD (mGal)	Weight
	EGM2008	5.3276	0.2195
Correct 2	EIGEN-6C4	4.9708	0.2522
CryoSat-2	SGG-UGM-2	5.0912	0.2404
	XGM2019e_2159	4.6529	0.2878
	EGM2008	5.7078	0.2252
HY-2A	EIGEN-6C4	5.3721	0.2541
	SGG-UGM-2	5.5554	0.2377
	XGM2019e_2159	5.0913	0.2830

Table 8. Weight proportion of different reference models with a marine depth less than 2000 m.

Table 9. The accuracy of the weighted fusion gravity anomalies with a marine depth less than 2000 m (unit: mGal).

Difference	Satellite	Min	Max	Mean	STD
Fusion-DTU17	CryoSat-2 HY-2A	-51.5867 -49.0245	45.9602 57.3946	0.9729 0.7653	4.6214 5.0686

5. Conclusions

In this paper, the influence of different reference gravity field models on the recovery of gravity anomalies using altimeter data is studied. The main conclusions are as follows:

- 1. HUST-Grace2016s, WHU-SWPU-GOGR2022S, and EGM2008 are utilized as reference fields to assess the accuracy of altimeter-derived gravity anomalies. The STD of the gravity anomalies for the two types of satellites is observed to decrease successively from 49 mGal to 31 mGal, and ultimately to 4 mGal. It is concluded that when recovering the marine gravity field using altimeter data, high-degree gravity field models should be prioritized as reference fields.
- 2. The effects of four different high-degree reference gravity field models on the recovery of gravity anomalies using altimeter data are analyzed. The results reveal that the utilization of these different high-degree models exerts minimal influence on the outcomes of the recovered gravity anomalies. In contrast, the evaluation based on shipborne data and DTU17 confirms that the XGM2019e_2159 model is optimal, which aligns with the reference gravity anomaly employed by the SDUST gravity anomaly model released by Shandong University of Science and Technology.
- 3. When using the same high-degree reference gravity field model, the gravity anomalies inverted by HY-2A are similar to those of CryoSat-2, which proves that HY-2A reached the world's most advanced level. Under the same conditions, the STD of gravity anomalies retrieved by CryoSat-2 is approximately 0.2 mGal smaller than that of HY-2A.
- 4. The accuracy of the altimeter data in restoring the marine gravity field on the shallow shore is low. When the marine depth is less than 2000 m, both CryoSat-2 and HY-2A using the XGM2019e_2159 model to restore the gravity field obtain the highest accuracies. Compared with EGM2008, the accuracy is improved by 0.6747 mGal and 0.6165 mGal, respectively. The weighted fusion method proposed in this paper can further improve the problem of the poor inversion accuracy of altimeter satellites in shallow water areas.

Author Contributions: Writing—original draft preparation, Y.H.; conceptualization, H.W.; supervision, F.Q. and H.W.; writing—review and editing, L.Q.; software, F.Z.; funding acquisition, F.Q. All authors have read and agreed to the published version of the manuscript.

Funding: This research was funded by the National Natural Science Foundation of China, grant number 42274013.

Remote Sens. 2024, 16, 3758 15 of 16

Data Availability Statement: Publicly available datasets were used in this study. The altimeter products were produced and distributed by AVISO (https://www.aviso.altimetry.fr/, accessed on 18 August 2024). The JAMSTEC shipborne data can be found here: https://www.godac.jamstec.go.jp/, accessed on 18 August 2024. DTU17 can be found here: https://ftp.space.dtu.dk/pub/, accessed on 18 August 2024. Reference Gravity Field Model can be found here: https://icgem.gfz-potsdam.de/tom_longtime, accessed on 18 August 2024.

Acknowledgments: We are very grateful to AVISO for providing the altimeter data and JAMSTEC for providing the shipborne gravity data. We are also thankful to DTU for the marine gravity anomaly models. Thanks to ICGEM for providing the reference gravity field.

Conflicts of Interest: The authors declare no conflicts of interest.

References

- 1. Zheng, W.; Xu, H.; Zhong, M.; Yuan, M.; Peng, B.; Zhou, X. Progress and Present Status of Research on Earth's Gravitational Field Models. *J. Geods. Geodyn.* **2010**, *30*, 83–91.
- 2. Sandwell, D.T.; Mueller, R.D.; Smith, W.H.F.; Garcia, E.; Francis, R. New Global Marine Gravity Model from CryoSat-2 and Jason-1 Reveals Buried Tectonic Structure. *Science* **2014**, *346*, 65–67. [CrossRef] [PubMed]
- 3. Li, Q.; Bao, L.; Shum, C. Altimeter-Derived Marine Gravity Variations Reveal the Magma Mass Motions within the Subaqueous Nishinoshima Volcano, Izu-Bonin Arc, Japan. *J. Geod.* **2021**, *95*, 46. [CrossRef]
- Hwang, C.; Chang, E.T.Y. Seafloor Secrets Revealed. Science 2014, 346, 32–33. [CrossRef]
- 5. Zehentner, N.; Mayer-Guerr, T. Precise Orbit Determination Based on Raw GPS Measurements. *J. Geod.* **2016**, *90*, 275–286. [CrossRef]
- 6. Mao, N.; Li, A.; Xu, J.; Qin, F.; Wu, M.; He, H.; Li, J. Marine Gravity Anomaly from Satellite Altimetry: Interpolation and Matching Navigation. *IEEE Trans. Geosci. Remote Sens.* **2023**, *61*, 5918919. [CrossRef]
- 7. Huang, M.; Liu, M.; Deng, K.; Ouyang, Y.; Lu, X.; Zhai, G.; Wu, T.; Chen, X. Test and correction of scale values for air-sea gravimeters using repeated survey lines. *Chin. J. Geophys.-Chin. Ed.* **2018**, *61*, 3160–3169.
- 8. Wang, B.; Wu, L.; Wu, P.; Li, Q.; Bao, L.; Wang, Y. Multidimensional Evaluation of Altimetry Marine Gravity Models with Shipborne Gravity Data from a New Platform Marine Gravimeter. *J. Mar. Sci. Eng.* **2024**, *12*, 1314. [CrossRef]
- 9. Chen, X.; Kong, X.; Zhou, R.; Zhang, S. Fusion of Altimetry-Derived Model and Ship-Borne Data in Preparation of High-Resolution Marine Gravity Determination. *Geophys. J. Int.* **2024**, *236*, 1262–1274. [CrossRef]
- 10. Wan, X.; Zhang, R.; Sui, X.; Chen, L. Analysis of Earth Gravity Field Detection Based on Satellite Data. *Spacecr. Eng.* **2017**, 26, 121–129.
- 11. Li, A.; Che, H.; Qin, F.; Huang, C.; Gong, W. Development and Prospect of Cold Atom Interferometry Gravimetry Measurement. *J. Nav. Univ. Eng.* **2021**, *33*, 1–7.
- 12. Che, H.; Li, A.; Fang, J.; Ge, G.; Gao, W.; Zhang, Y.; Liu, C.; Xu, J.; Chang, L.; Huang, C.; et al. Ship-borne dynamic absolute gravity measurement based on cold atom gravimeter. *Acta Phys. Sin.* **2022**, *71*, 113701. [CrossRef]
- 13. Sandwell, D.T.; Smith, W.H.F. Marine Gravity Anomaly from Geosat and ERS 1 Satellite Altimetry. *J. Geophys. Res.* **1997**, 102, 10039–10054. [CrossRef]
- 14. Sandwell, D.T.; Smith, W.H.F. Global Marine Gravity from Retracked Geosat and ERS-1 Altimetry: Ridge Segmentation versus Spreading Rate. *J. Geophys. Res.* **2009**, *114*, B1. [CrossRef]
- 15. Andersen, O.B.; Knudsen, P. Global Marine Gravity Field from the ERS-1 and Geosat Geodetic Mission Altimetry. *J. Geophys. Res.* **1998**, *103*, 8129–8137. [CrossRef]
- 16. Andersen, O.B. The DTU10 Global Gravity Field and Mean Sea Surface—Improvements in the Arctic. In Proceedings of the 2nd IGFS Meeting, Fairbanks, AK, USA, 20–22 September 2010.
- 17. Wan, X.; Annan, R.; Wang, W. Assessment of HY-2A GM Data by Deriving the Gravity Field and Bathymetry over the Gulf of Guinea. *Earth Planets Space* **2020**, 72, 151. [CrossRef]
- 18. Zhu, C.; Guo, J.; Hwang, C.; Gao, J.; Yuan, J.; Liu, X. How HY-2A/GM Altimeter Performs in Marine Gravity Derivation: Assessment in the South China Sea. *Geophys. J. Int.* **2019**, 219, 1056–1064. [CrossRef]
- 19. Li, J.; Sideris, M.G. Marine Gravity and Geoid Determination by Optimal Combination of Satellite Altimetry and Shipborne Gravimetry Data. *J. Geod.* **1997**, *71*, 209–216. [CrossRef]
- 20. Zhu, C.; Yang, L.; Bian, H.; Li, H.; Guo, J.; Liu, N.; Lin, L. Recovering Gravity from Satellite Altimetry Data Using Deep Learning Network. *IEEE Trans. Geosci. Remote Sens.* **2023**, *61*, 5911311. [CrossRef]
- 21. Liu, Q.; Xu, K.; Jiang, M.; Wang, J. Preliminary Marine Gravity Field from HY-2A/GM Altimeter Data. *Acta Oceanol. Sin.* 2020, 39, 127–134. [CrossRef]
- 22. Zaki, A.; Mansi, A.H.; Selim, M.; Rabah, M.; El-Fiky, G. Comparison of Satellite Altimetric Gravity and Global Geopotential Models with Shipborne Gravity in the Red Sea. *Mar. Geod.* **2018**, *41*, 258–269. [CrossRef]
- 23. Li, Q.; Bao, L.; Wang, Y. Accuracy Evaluation of Altimeter-Derived Gravity Field Models in Offshore and Coastal Regions of China. *Front. Earth Sci.* **2021**, *9*, 722019. [CrossRef]

24. Wang, B.; Wu, L.; Li, Q.; Bao, L.; Wang, Y. Estimating the True Spatial Resolution of Satellite Altimeter-Derived Gravity Field Models with Shipborne Data in the South China Sea. *Appl. Geophys.* **2023**, *20*, 51–61. [CrossRef]

- 25. Annan, R.F.; Wan, X. Recovering Marine Gravity Over the Gulf of Guinea From Multi-Satellite Sea Surface Heights. *Front. Earth Sci.* **2021**, *9*, 700873. [CrossRef]
- 26. Zhang, W.; Zheng, W.; Ku, F.; Li, Z.; Liu, Z. Research Progress and Prospect of Global Marine Gravity Field Model. *Sci. Surv. Mapp.* **2020**, *45*, 16–30.
- 27. Hwang, C.; Hsu, H.-Y.; Jang, R.-J. Global Mean Sea Surface and Marine Gravity Anomaly from Multi-Satellite Altimetry: Applications of Deflection-Geoid and Inverse Vening Meinesz Formulae. *J. Geod.* **2002**, *76*, 407–418. [CrossRef]
- 28. Hwang, C. Inverse Vening Meinesz Formula and Deflection-Geoid Formula: Applications to the Predictions of Gravity and Geoid over the South China Sea. *J. Geod.* **1998**, 72, 304–312. [CrossRef]
- 29. Wan, X.; Yu, J. Accuracy Analysis of the Remove-Restore Process in Inverse Stokes Formula. *Geomat. Inf. Sci. Wuhan Univ.* **2012**, 37, 77–80.
- 30. Li, Z.; Guo, J.; Ji, B.; Wan, X.; Zhang, S. A Review of Marine Gravity Field Recovery from Satellite Altimetry. *Remote Sens.* **2022**, *14*, 4790. [CrossRef]
- 31. Li, Z. Satellite Radar Altimeter Waveform Retracking of Waveform Derivative Method and Derivation of Gravity Anomalies. Mater's Dissertation, Shandong University of Science and Technology, Qingdao, China, 2020.
- 32. Zhang, S. Research on Determination of Marine Gravity Anomalies from Multi-Satellite Altimeter Data. Ph.D. Dissertation, Wuhan University, Wuhan, China, 2016.
- 33. Along-Track Level-2+ (L2P) SLA Product Handbook; CNES Paris: Paris, France, 2017.
- 34. Zhu, C.; Guo, J.; Yuan, J.; Li, Z.; Liu, X.; Gao, J. SDUST2021GRA: Global Marine Gravity Anomaly Model Recovered from Ka-Band and Ku-Band Satellite Altimeter Data. *Earth Syst. Sci. Data* 2022, 14, 4589–4606. [CrossRef]
- 35. Zhang, S.; Sandwell, D.T.; Jin, T.; Li, D. Inversion of Marine Gravity Anomalies over Southeastern China Seas from Multi-Satellite Altimeter Vertical Deflections. *J. Appl. Geophys.* **2017**, *137*, 128–137. [CrossRef]
- 36. Zhu, C.; Guo, J.; Gao, J.; Liu, X.; Hwang, C.; Yu, S.; Yuan, J.; Ji, B.; Guan, B. Marine Gravity Determined from Multi-Satellite GM/ERM Altimeter Data over the South China Sea: SCSGA V1.0. *J. Geod.* 2020, 94, 50. [CrossRef]
- 37. Tscherning, C.C.; Rapp, R.H. Closed Covariance Expressions for Gravity Anomalies, Geoid Undulations, and Deflections of the Vertical Implied by Anomaly Degree Variance Models; Division of Geodetic Science: Columbus, OH, USA, 1974.

Disclaimer/Publisher's Note: The statements, opinions and data contained in all publications are solely those of the individual author(s) and contributor(s) and not of MDPI and/or the editor(s). MDPI and/or the editor(s) disclaim responsibility for any injury to people or property resulting from any ideas, methods, instructions or products referred to in the content.